DOI: 10.6060/mhc246168t

Dyades of 5,15-Diphenylporphyrin with Pyrene

Uliana A. Gerasimova,[a] Artemiy K. Ershov,[b] Alexander S. Kuvakin,[a] Andrey Y. Chernyadiev,[a] Dmitriy N. Kuznetsov,[b] Sergey N. Ryagin,[c] Ilya A. Zamilatskov,[a] and Vladimir S. Tyurin[a@]

[a]*A.N. Frumkin Institute of Physical Chemistry and Electrochemistry, Russian Academy of Sciences, 119071 Moscow, Russia*
[b]*A.N. Kosygin Russian State University, 119071 Moscow, Russia*
[c]*Non-state private educational institution of higher professional education Moscow University for Industry and Finance «Synergy», 125190 Moscow, Russia*
[@]*Corresponding author E-mail: vst-1970@mail.ru*

New dyads consisting of 5,15-diphenylporphyrin and pyrene chromophores were synthesized through the Suzuki coupling of halogenated porphyrins with pyreneboronic acid. Two different types of dyads were obtained: one with a direct connection between the macrocycles, and the other with an ethene bridge in between them. The free bases as well as the nickel and zinc complexes of these dyads were investigated using electron absorption and emission spectroscopy. A weak interaction was observed between the components in the ground state in the directly linked dyads, while a stronger interaction was found in the ethene-bridged ones. In the excited state, energy flows from pyrene to porphyrin chromophore in both types of dyad, but with different efficiencies depending on the metal complex or free base porphyrin used as a component of the dyad. DFT calculations provide insights into the structural features and interactions in these dyads. The obtained dyads may be of interest as potential photosensitizers and ratiometric luminescent sensors based on their dual blue and red luminescence.

Keywords Porphyrins, pyrene, dyads, Suzuki reaction, photosensitizers, fluorescence, sensors.

Диады 5,15-дифенилпорфирина с пиреном

У. А. Герасимова,[a] А. К. Ершов,[b] А. С. Кувакин,[a] А. Ю. Чернядьев,[a] Д. Н. Кузнецов,[b] С. Н. Рягин,[c] И. А. Замилацков,[a] В. С. Тюрин[a@]

[a]*Институт физической химии и электрохимии им. А.Н. Фрумкина РАН, 119071 Москва, Российская Федерация*
[b]*ФГБОУ ВО «Российский государственный университет им. А.Н. Косыгина, 119071 Москва, Российская Федерация*
[c]*НОЧУ ВО Московский финансово-промышленный университет «Синергия» 125190 Москва, Российская Федерация*
[@]*E-mail: vst-1970@mail.ru*

Новые диады, состоящие из хромофоров 5,15-дифенилпорфирина и пирена, были синтезированы путем соединения галогенированных порфиринов по методу Сузуки с пиренбороновой кислотой. Были получены два различных типа диад: одна с прямой связью между макроциклами, а другая с этеновым мостиком между ними. Свободные основания, а также комплексы никеля и цинка в этих диадах были исследованы с помощью электронной абсорбционной и эмиссионной спектроскопии. В непосредственно связанных диадах наблюдалось слабое взаимодействие между компонентами, в то время как в диадах с этеновым мостиком было обнаружено более сильное взаимодействие. В возбужденном состоянии энергия передается от пирена к порфириновому хромофору в обоих типах диад, но с разной эффективностью. Расчеты методом DFT позволили получить представление о структурных особенностях и деталях взаимодействий в этих диадах. Полученные диады могут представлять интерес в качестве потенциальных фотосенсибилизаторов и рациометрических люминесцентных сенсоров, основанных на их двойной синей и красной люминесценции.

Ключевые слова: Порфирины, пирен, диады, реакция Сузуки, фотосенсибилизаторы, флуоресценция, сенсоры.

Introduction

Aromatic macrocycles represent chromophores with plane rigid geometry leading to good luminescent properties. Fused benzene aromatic hydrocarbons called as polycyclic aromatic hydrocarbons (PAHs) absorb light in UV range and emit it in blue visible range. Tetrapyrrolic macrocycles with 18π aromatic system with absorption at near UV and visible range emit in green and red. Combining tetrapyrroles and PAHs leads to nonsymmetric dyads attracting an attention of researchers due to the fact that, unlike single components, they acquire new or enhance already existing useful properties.[1, 2] Thus, the extinction coefficient increases, while the absorption shifts to the red region, which is crucial for the photodynamic therapy (PDT) in order the absorption to fall within the tissue transparency window.[3] In some cases, the absorption approaches panchromatic, which is useful for dye sensitized solar cells. The two-photon absorption cross-section increases dramatically in the conjugated porphyrin dyads, which is also used in PDT and optical diagnostics.[4,5] Among the new properties is the possibility of transferring energy and/or an electron between the components of the dyad in an excited state.[6] Thus, combining porphyrins and PAHs into the dyad, can lead to the new properties, rather than sum of properties of components. Among these new properties of the dyads are energy or electron transfer processes.[7-13] These dyads are widely used as photosensitizers for photo therapy[14-20] and also as sensors,[21,22] in photovoltaics,[23-31] nonlinear photonics,[32] up-conversion,[33,34] *etc*. A typical representative of PAH is pyrene with 14π aromatic system. High affinity of pyrene to carbon materials allowed to use them to attach to the surface of carbon nanotubes, fullerenes and grapheme.[35-40] Pyrene is widely used as valuable fluorescent probes because it possesses a high quantum yield and lifetime of fluorescence.[41] Porphyrin attachment significantly modifies electronic photonic and sensor properties of pyrene.[42,43] The sensor capabilities of the porphyrin-pyrene dyad are significantly enhanced due to the ability to use the ratio of the blue luminescence from the pyrene fragment and the red luminescence from the porphyrin chromophore.[43]

Significant factor in the interaction of components of the dyad is a place of attachment.[44] Substituents at *meso*-position have stronger influence on the tetrapyrrole π-electron system. Various dyads were studied where PAH fragments have been attached to the *meso*-position of porphyrins, including pyrene, naphthalene, perylene, coronene.[45] However, direct attachment of aromatic fragments to the porphyrin does not provide conjugation between chromophores due to their orthogonal mutual orientation caused by sterical hindrances at *meso*-position. Subsequent fusion of the PAN substituent with β-position can solve the problem but the components lose their individuality. Alternatively, the conjugation of the components of the dyad can be achieved using appropriate unsaturated bridge. Previously, we have developed methods for the synthesis and investigated properties of porphyrin dyads connected by various bridges such as 1,3-butadiene,[46] butenine[47] and azine bridges.[48,49] In this work, dyads of the 5,15-diphenylporphyrin and pyrene were obtained using both direct attachment and ethene bridging. *meso*-Ethene-bridged porphyrin-pyrene dyads have not been previously reported, but this type of linkage promises strong conjugation and a high degree of interaction between the chromophores. For comparison, the same chromophores were also linked directly without conjugation.

Experimental

General

Reactions were carried out under argon atmosphere using commercially available reagents that were purchased and used as received. Heating reaction vessels was performed with oil bath. Silica gel 40/60 was used for column and flash chromatography. Preparative thin layer chromatography (TLC) was performed using glass plates coated with 5–40 μm silica gel (5 mm thick). ^{1}H and ^{13}C NMR spectra were recorded with a Bruker Avance III 600 MHz spectrometer at 303K in $CDCl_3$. Chemical shifts are reported relative to signals of residual protons of solvents ($CDCl_3$ – 7.26 ppm). The assignment of the resonances in the ^{1}H NMR spectra was achieved by the use of COSY and HSQC techniques. The LDI-TOF mass-spectra were obtained on a Ultraflex-II mass spectrometer (Bruker Daltonics) in a positive ion mode using reflection mode (20 mV target voltage) without matrix. Electronic absorption spectra were recorded with U-2900 (Hitachi) spectrophotometer in quartz rectangular cells of 10 mm path length. The photoluminescence spectra were recorded on the Fluorolog-3 spectrofluorometer (HORIBA Jobin Yvon S.A.S.). The excitation source was a 450 W xenon lamp with Czerny-Turner double monochromators; an R928 photomultiplier and an InGaAs near-IR detector were used to detect the signals.

Synthesis

Pyrene-1-boronic acid was obtained from commercial sources.

2,2'-Dipyrromethane was synthesized *via* a slightly modified procedure by Lindsey.[50] A suspension of paraformaldehyde (0.375 g, 12.5 mmol) in pyrrole (43 mL, 0.62 mol) was placed in a 100-mL flask equipped with a reflux condenser and argon was bubbled through the mixture for 5 min. The mixture was then stirred and heated to 60 °C. After that, the heating was removed and TFA (0.1 mL, 1.3 mmol) was added dropwise via syringe. The temperature rise about 10 °C was observed, the solution turned yellow, and the paraformaldehyde was completely dissolved. Reaction mixture was then stirred for an hour without heating and quenched by adding KOH pellets (0.5 g, 0.09 mmol) and stirring for 10 min. Then the reaction mixture was passed through a short silica pad and distilled in a Kugelrohr starting at 10 mmHg, to remove excess pyrrole, followed by distillation at 0.1 mmHg with gradually increasing bath temperature from 120 to 180 °C. The product was obtained as colorless crystals in a yield of 1.33 g (73%), mp 75 °C. ^{1}H NMR (600 MHz, $CDCl_3$, 303 K) δ ppm: 3.99 (2H, s, CH_2), 6.07 (2H, m), 6.18 (2H, q, J = 2.9 Hz), 6.67 (2H, m), 7.84 (2H, br.s, NH).

*5,15-Diphenylporphyrin (**1**)* was synthesized by Mc Donald [2+2] condensation of dipyrromethane and benzaldehyde with slightly modified procedure of Therien.[51] A 1 L flask filled with argon and shielded from light with aluminum foil was charged with dipyrromethane (0.59 g, 4 mmol), benzaldehyde (0.41 mL, 4 mmol), and 0.75 L of dry methylene chloride. The solution was deoxygenated with argon bubbling for 10 min. Trifluoroacetic acid (48 μL, 0.62 mmol) was added dropwise via syringe, and the solution was stirred for 3 h at room temperature. Then the solution of DDQ (1.4 g, 5 mmol) in 10 mL THF was added to the reaction mixture, which was further stirred for an hour. After that,

the mixture was neutralized with 5 mL of triethylamine and concentrated in rotary evaporator to 50 mL, passed through a silica pad and purified by column chromatography on silica gel column (20×3 cm) with eluent CH_2Cl_2–C_6H_6 1:1. The product was obtained as purple crystals in a yield of 0.59 g (63%). ^{1}H NMR (600 MHz, $CDCl_3$, 303 K) δ ppm: –3.07 (s, 2H, NH), 7.84 (6H, m, Ph), 8.31 (4H, m, Ph), 9.11 (4H, d, J = 4.5 Hz, β-H), 9.42 (4H, d, J = 4.5 Hz, β-H), 10.34 (2H, s, *meso*-H). UV-Vis (CH_2Cl_2) λ_{max} ($A_{rel.}$) nm: 412 (1.00), 508 (0.035), 543 (0.006), 580 (0.014), 636 (0.003).

*5-Bromo-10,20-diphenylporphyrin (**2**)* was synthesized with modified procedure of Liebeskind.[52] 5,15-Diphenylporphyrin (**1**) (0.29 g, 0.63 mmol) was dissolved in a mixture of CH_2Cl_2 and MeOH (9:1, 150 mL) and NBS (0.11 g, 0.63 mmol) was added. The reaction mixture was stirred at room temperature for 15 min and then quenched with acetone (15 mL). The solvent was evaporated and the residue was purified using gradient column chromatography with a CH_2Cl_2–hexane system (1:4 to 2:1). The yield of **2** was 0.28 g (81%). ^{1}H NMR (600 MHz, $CDCl_3$, 303 K) δ ppm: -3.08 (s, 2H, NH), 7.8 (6H, m, Ph), 8.22 (4H, m, Ph), 8.97 (4H, d, J = 4.7 Hz, β-H), 9.31 (2H, d, J = 4.7 Hz, β-H), 9.75 (2H, d, J = 4.7 Hz, β-H), 10.19 (1H, s, *meso*-H). ^{13}C NMR (150 MHz, $CDCl_3$, 303 K) δ ppm: 141.8, 135.2, 132.9, 132.6, 132.3, 128.5, 127.5, 120.9, 106.1, 103.9. UV-Vis (CH_2Cl_2) λ_{max} ($A_{rel.}$) nm: 414 (1.00), 511 (0.052), 545 (0.017), 587 (0.017), 643 (0.012).

*Zn(II) 5-Bromo-10,20-diphenylporphyrin (**4**)* was synthesized according to Liebeskind.[52] A solution of 5-bromo-10,20-diphenylporphyrin (**2**) (0.33 g, 0.61 mmol) in chloroform (80 mL) was added to a solution of zinc acetate (0.66 g, 3 mmol) in methanol (40 mL), and refluxed for an hour. Then the reaction mixture was allowed to cool and poured in water (0.2 L), extracted with CH_2Cl_2 (100 mL) and dried over sodium sulfate. The solution was passed through a silica pad, and the solvent was evaporated, yielding 0.31 g (83%) of the product. ^{1}H NMR (600 MHz, $CDCl_3$, 303 K) δ ppm: 7.80 (6H, m, Ph), 8.21 (4H, m, Ph), 9.04 (4H, d, J = 4.5 Hz, β-H), 9.35(2H, d, J = 4.5 Hz, β-H), 9.81(2H, d, J = 4.5 Hz, β-H), 10.21 (1H, s, *meso*-H). UV-Vis (CH_2Cl_2) λ_{max} ($A_{rel.}$) nm: 416 (1.00), 546 (0.04).

*Ni(II) 5,15-Diphenylporphyrin (NiDPP) (**5**).* 5,15-Diphenylporphyrin (**1**) (0.3 g, 0.65 mmol) and $Ni(OAc)_2$ (1.3 g, 7.7 mmol) were dissolved in DMF (20 mL), and the solution was refluxed for 12 h. After that the mixture was poured in water (0.4 L) and extracted with CH_2Cl_2 (100 mL), washed with water (3×100 mL) and dried over Na_2SO_4. The solvent was evaporated, and the product was further purified by column chromatography using CH_2Cl_2 as an eluent. The yield of the product (**5**) was 0.3 g (90%). ^{1}H NMR (600 MHz, $CDCl_3$, 303 K) δ ppm: 7.75 (6H, m, Ph), 8.09 (4H, m, Ph), 8.97 (4H, d, J = 4.5 Hz, β-H), 9.22 (4H, d, J = 4.5 Hz, β-H), 9.97 (2H, s, *meso*-H). UV-Vis (CH_2Cl_2) λ_{max} ($A_{rel.}$) nm: 403 (1.00), 519 (0.074), 551 (0.035).

*Ni(II) 5-Formyl-10,20-diphenylporphyrin (**6**)* was obtained *via* the Vilsmeier-Haack formylation reaction of Ni(II) 5,15-diphenylporphyrin (**5**).[53] Ni(II) 5,15-diphenylporphyrin (**5**) (50 mg, 0.096 ммоль) was dissolved in 1,2-dichloroethane (10 mL). Then, 3.5 mL of the Vilsmeier reagent, obtained from 2 mL (25.8 mmol) of DMF and 2 mL (21.5 mmol) $POCl_3$, was dropwise added to the solution of **5** with rapid stirring. The reaction was stirred for 4 h at 50 °C, then the reaction mixture was poured in water (50 mL) and extracted with CH_2Cl_2 (50 mL). The organic phase was washed with water (3×30 mL), saturated solution of $NaHCO_3$ (30 mL) and dried over Na_2SO_4. The solvent was evaporated in vacuum and the residue was purified using column chromatography in the CH_2Cl_2–petroleum ether (2:1) eluent. The product was crystallized from petroleum ether, yielding 45 mg (86%) of **6**. ^{1}H NMR (600 MHz, $CDCl_3$, 303 K) δ ppm: 7.72 (6H, m, Ph), 7.97 (4H, m, Ph), 8.73 (2H, d, J = 4.5 Hz, β-H), 8.89 (2H, d, J = 4.5 Hz, β-H), 9.01(2H, d, J = 4.5 Hz, β-H), 9.68 (1H, s, *meso*-H) 9.84 (2H, d, J = 4.5 Hz, β-H), 12.10 (1H, s, CHO). UV-Vis (CH_2Cl_2) λ_{max} ($A_{rel.}$) nm: 423 (1.00), 551 (0.055), 582 (0.071), 599 (0.082).

*Ni(II) 5-(2-iodoethenyl)-10,20-diphenylporphyrin (**7**)* was synthesized from Ni(II) 5-formyl-10,20-diphenylporphyrin (**6**) using slightly modified procedure[47] of the Takai reaction.[54] $CrCl_2$ (300 mg, 2.44 mmol) was dried by heating at 180–200 °C under vacuum 0.1 mmHg for 10 min, then the flask was allowed to cool, filled with argon and dry deoxygenated THF (3 mL) was added. The resulted slurry was stirred for 15 min. To another flask containing Ni(II) 5-formyl-10,20-diphenylporphyrin (**6**) (50 mg, 0.091 mmol), 6 mL of dry THF was added, followed by CHI_3 (220 mg, 0.56 mmol) and the mixture was stirred for 10 min, then the solution was dropwise added to the $CrCl_2$ suspension over a period of 10 min. The reaction mixture was then stirred at room temperature for 3 h. The solution changed from purple to dark red over time. The reaction mixture was subsequently passed through a short silica plug using diethyl ether as an eluent. Then the solvent was evaporated in vacuum, the residue was dissolved in CH_2Cl_2 (30 mL) and washed with water (3×30 mL) and dried over Na_2SO_4. Then the solvent was evaporated in vacuum, and the residue was dissolved in minimum amount of diethyl ether and treated with tetrabutylammonium fluoride (TBAF) (1 mL, 1 M in THF) to remove excess of CHI_3 for 15 min. Then, the solution was passed through a short silica plug using diethyl ether as an eluent, the solvent was evaporated in vacuum, the residue dissolved in CH_2Cl_2 (30 mL), washed with water (3×20 mL) and dried over Na_2SO_4. Then the solvent was evaporated in vacuum, and the residue was subjected to column chromatography using CH_2Cl_2/petroleum ether (2:3) as an eluent, yielding 33 mg (54%) of **7**. ^{1}H NMR (600 MHz, $CDCl_3$) δ ppm: 9.71 (1H, s, *meso*-H), 9.63 (1H, d, J = 14.68 Hz, I-C*H*=CH), 9.68 (2H, d, J = 4.95 Hz, *β*-H), 9.06 (2H, d, J = 4.76 Hz, *β*-H), 9.68 (2H, d, J = 4.95 Hz, *β*-H), 8.85 (2H, d, J = 4.88 Hz, *β*-H), 8.82 (2H, d, J = 4.70 Hz, *β*-H), 8.01 (4H, m, Ph), 7.74 (6H, m, Ph), 6.75 (1H, d, J = 14.68 Hz, I-CH=C*H*). ^{13}C NMR (150 MHz, $CDCl_3$, 303 K) δ ppm: 86.60, 104.88, 114.68, 118.68, 126.96, 127.85, 130.91, 132.35, 132.73, 133.70, 133.84, 140.56, 140.63, 142.22, 142.67, 143.89. UV-Vis (CH_2Cl_2) λ_{max} ($A_{rel.}$) nm: 419 (1.00), 533 (0.088).

*5-(2-Iodoethenyl)-10,20-diphenylporphyrin (**8**).* Ni(II) 5-(2-iodoethenyl)-10,20-diphenylporphyrin (**7**) (50 mg, 0.075 mmol) was dissolved in 10%vv sulfuric acid in trifluoroacetic acid (10 mL). The mixture was stirred at room temperature for 30 min and poured in ice water (100 mL), extracted with CH_2Cl_2 (50 mL) and washed with water (2×20 mL), saturated $NaHCO_3$ (20 mL) and dried over Na_2SO_4. The solvent was evaporated at reduced pressure and the residue was purified by column chromatography on silica gel, eluting with CH_2Cl_2/petroleum ether (3:2). The yield of **8** was 20 mg (44%). ^{1}H NMR (600 MHz, $CDCl_3$) δ ppm: 7.83 (6H, m, Ph in Porphyrin), 8.25 (4H, m, Ph in Porphyrin), 7.19 (1H, d, J=15.72 Hz, C^{2}H Ethenyl), 9.0 (4H, m, β-H in Porphyrin), 9.30 (2H, d, J = 3.83 Hz, β-H in Porphyrin), 9.44 (2H, d, J = 4.22 Hz, β-H in Porphyrin), 9.96 (1H, d, J = 15.72 Hz, C^{1}H Ethenyl), 10.19 (1H, s, *meso*-H in Porphyrin) UV-Vis (CH_2Cl_2) λ_{max} ($A_{rel.}$) nm: 416 (1.00), 513 (0.043), 549 (0.024), 589 (0.019), 645 (0.011). LDI *m/z*: found 487.209, calc. for $[M\text{-}I]^+$ $C_{34}H_{23}N_4$: 487.192.

*Zn(II) 5-(pyrene-1-yl)-10,20-diphenylporphyrin (**11**).* Zn(II) 5-bromo-10,20-diphenylporphyrin (**4**) (24 mg, 0.04 mmol), pyrene-1-boronic acid (**9**) (15 mg, 0.06 mmol), $Pd(dba)_2$ (1.1 mg, 0.0019 mmol), CyJohnPhos (1.4 mg, 0.004 mmol), Cs_2CO_3 (52 mg, 0.16 mmol) were loaded in the flask filled with argon, then THF (8 mL) and water (0.3 mL) were added and stirred at 60 °C for a day. Then the solvent was evaporated and the residue was purified by column chromatography on silica gel, eluting with CH_2Cl_2. The yield of **11** was 20.4 mg (71%). ^{1}H NMR (600 MHz, $CDCl_3$, 303 K) δ ppm: 7.43 (1H, d, J = 9.41 Hz, Pyrenyl), 7.67 (1H, d, J = 9.41 Hz, Pyrenyl), 7.78 (6H, m, Ph in Porphyrin), 8.07 (2H, m, Pyrenyl), 8.27 (4H, m, Ph in Porphyrin), 8.34 (2H, m, Pyrenyl), 8.43 (1H, d, J = 9.20 Hz, Pyrenyl), 8.54 (1H, d, J = 7.56 Hz, Pyrenyl), 8.65 (2H, d, J = 4.56 Hz, β-H in Porphyrin), 8.83 (1H, d, J = 7.56 Hz, Pyrenyl), 8.92 (2H, d, J = 4.56 Hz, β-H in Porphyrin),

9.13 (2H, d, *J* = 4.46 Hz, β-H in Porphyrin), 9.46 (2H, d, *J* = 4.46 Hz, β-H in Porphyrin), 10.43 (1H, s, *meso*-H in Porphyrin). UV-Vis (CH_2Cl_2) λ_{max} ($A_{rel.}$) nm: 272 (0.700), 420 (1.00), 551 (0.427), 590 (0.008). LDI *m/z*: found 725.174, calc. for $[M+H]^+$ $C_{48}H_{29}N_4Zn$: 725.168.

*5-(Pyrene-1-yl)-10,20-diphenylporphyrin (**12**).* Zn(II) 5-(pyrene-1-yl)-10,20-diphenylporphyrin (**11**) (20 mg, 0.028 mmol) was dissolved in choroform (5 mL) and TFA (0.02 mL) was added. The mixture was stirred at 50 °C for 10 min, then poured in saturated $NaHCO_3$ (40 mL), extracted with CH_2Cl_2 (30 mL), the extract was washed with saturated $NaHCO_3$ (40 mL) and dried over Na_2SO_4. The solvent was evaporated at reduced pressure and the residue was purified by column chromatography on silica gel, eluting with CH_2Cl_2/petroleum ether (1:1). The yield of **12** was 18 mg (99%). ^{1}H NMR (600 MHz, $CDCl_3$, 303 K) δ ppm: –2.74 (s, 2H, NH), 7.43 (1H, d, *J* = 9.37 Hz, Pyrenyl), 7.69 (1H, d, *J* = 9.52 Hz, Pyrenyl), 7.78 (6H, m, Ph in Porphyrin), 8.00 (2H, m, Pyrenyl), 8.27 (4H, m, Ph in Porphyrin), 8.36 (2H, m, Pyrenyl), 8.43 (1H, d, *J* = 9.14 Hz, Pyrenyl), 8.54 (3H, m, β-H in Porphyrin and H in Pyrenyl), 8.82 (3H, m, β-H in Porphyrin and H in Pyrenyl), 9.10 (2H, d, *J* = 4.54 Hz, β-H in Porphyrin), 9.40 (2H, d, *J* = 4.54 Hz, β-H in Porphyrin), 10.3 (1H, s, *meso*-H in Porphyrin). ^{13}C NMR (150 MHz, $CDCl_3$, 303 K) δ ppm: 105.19, 118.20, 119.79, 122.69, 124.10, 124.64, 125.31, 125.58, 126.30, 126.82, 127.25, 127.64, 127.71, 127.72, 128.05, 130.83, 131.47, 131.78, 132.68, 133.57, 134.65, 134.68, 137.36, 141.66. UV-Vis (CH_2Cl_2) λ_{max} ($A_{rel.}$) nm: 413 (1.00), 541 (0.043). LDI *m/z*: found 663.263, calc. for $[M+H]^+$ $C_{48}H_{31}N_4$: 663.254.

*Ni(II) 5-(pyrene-1-yl)-10,20-diphenylporphyrin (**13**).* 5-(Pyrene-1-yl)-10,20-diphenylporphyrin (**12**) (18 mg, 0.027 mmol), and $Ni(OAc)_2{\cdot}4H_2O$ (94 mg, 0.53 mmol) were stirred in DMF (2 mL) at 150 °C for an hour. Then the mixture was poured in water (50 mL), extracted with CH_2Cl_2 (30 mL), washed with water (2×20 mL) and dried over Na_2SO_4. Then the solvent was evaporated and the residue was purified by column chromatography on silica gel, eluting with CH_2Cl_2/petroleum ether (1:1). The yield of **13** was 19 mg (97%). ^{1}H NMR (600 MHz, $CDCl_3$, 303 K) δ ppm: 7.31 (1H, d, *J* = 9.41 Hz, in Pyrenyl), 7.78 (7H, m, Ph in porphyrin and H in Pyrenyl), 8.10 (6H, m, Ph in porphyrin and H in Pyrenyl), 8.32 (2H, m, in Pyrenyl), 8.37 (1H, d, *J* = 9.12 Hz, in Pyrenyl), 8.49 (3H, m, β-H in porphyrin and H in Pyrenyl), 8.68 (1H, d, *J* = 7.70 Hz, in Pyrenyl), 8.73 (2H, d, *J* = 4.87 Hz, β-H in porphyrin), 8.94 (2H, d, *J* = 4.87 Hz, β-H in porphyrin), 9.20 (2H, d, *J* = 4.76 Hz, β-H in porphyrin), 9.92 (1H, s, *meso*-H in porphyrin). ^{13}C NMR (150 MHz, $CDCl_3$, 303 K) δ ppm: 104.96, 114.07, 117.30, 118.85, 122.91, 124.14, 124.59, 125.29, 125.53, 126.26, 126.86, 126.94, 127.59, 127.62, 127.75, 128.02, 130.83, 131.43, 131.69, 131.93, 132.21, 132.32, 132.38, 132.61, 132.98, 133.77, 135.86, 140.96, 142.88, 142.92, 142.98, 143.38 UV-Vis (CH_2Cl_2) λ_{max} ($A_{rel.}$) nm: 242 (0.395), 274 (0.215), 340 (0.142), 409 (1.00), 521 (0.088), 550 (0.028). LDI *m/z*: found 719.187, calc. for $[M+H]^+$ $C_{48}H_{29}N_4Ni$: 719.174.

*Ni(II) 5-(2-(pyrene-1-yl)ethenyl)-10,20-diphenylporphyrin (**14**).* Ni(II) 5-(2-iodoethenyl)-10,20-diphenylporphyrin (**7**) (10 mg, 0.015 mmol), pyrene-1-boronic acid (**9**) (16 mg, 0.065 mmol), $PdCl_2$dppf (2 mg, 0.0027 mmol), K_3PO_4 (20 mg, 0.094 mmol) were loaded in the flask filled with argon, then 1,4-dioxane (1 mL) and water (0.2 mL) were added and stirred at 40 °C for an 1 h. Then the mixture was poured in water (30 mL), extracted with CH_2Cl_2 (2×20 mL), washed with water (2×20 mL) and dried over Na_2SO_4. Then the solvent was evaporated and the residue was purified by column chromatography on silica gel, eluting with CH_2Cl_2/petroleum ether (1:2). The yield of **14** was 7.5 mg (68%). ^{1}H NMR (600 MHz, $CDCl_3$, 303 K) δ ppm: 7.74 (6H, m, Ph in Porphyrin), 7.98 (1H, d, *J* = 15.60 Hz, C^{2}H Ethenyl), 8.00 (1H, t, *J* = 7.57 Hz, Pyrenyl), 8.01 (5H, m, Ph in Porphyrin and H in Pyrenyl), 8.17 (3H, m, Pyrenyl), 8.23 (1H, d, *J* = 7.76 Hz, Pyrenyl), 8.40 (2H, m, Pyrenyl), 8.84 (2H, d, *J* = 4.72 Hz, β-H in Porphyrin), 8.87 (1H, d, *J* = 7.93 Hz, Pyrenyl), 8.91 (2H, d, *J* = 4.88 Hz, β-H in Porphyrin), 9.1 (2H, d, *J* = 4.72 Hz, β-H in Porphyrin), 9.60 (2H, d, *J* = 4.88 Hz, β-H in Porphyrin), 9.63 (1H, d, *J* = 15.60 Hz, C^{1}H Ethenyl), 9.73 (1H, s, *meso*-H in Porphyrin). ^{13}C NMR (150 MHz, $CDCl_3$, 303 K) δ ppm: 104.52, 115.57, 118.60, 122.96, 123.47, 124.99, 125.24, 125.33, 125.51, 126.12, 126.98, 128.34, 130.47, 131.45, 131.59, 132.22, 132.65, 132.68, 133.71, 140.74, 141.50, 142.02, 142.12, 142.44, 142.68. UV-Vis (CH_2Cl_2) λ_{max} ($A_{rel.}$) nm: 226 (5.4), 427 (1.00), 535 (0.128), 583(0.099). LDI *m/z*: found 745.206, calc. for $[M+H]^+$ $C_{50}H_{31}N_4Ni$: 745.190.

*5-(2-(Pyrene-1-yl)ethenyl)-10,20-diphenylporphyrin (**15**).* 5-(2-Iodoethenyl)-10,20-diphenylporphyrin (**8**) (10 mg, 0.016 mmol), pyrene-1-boronic acid (**9**) (10 mg, 0.04 mmol), K_3PO_4 (9 mg, 0.042 mmol) were loaded in the flask filled with argon, then 1,4-dioxane (4 mL) and water (0.8 mL) were added and stirred at room temperature for 5 min. Then $PdCl_2$dppf (2.4 mg, 0.0032 mmol) was added and the mixture was stirred for 8 h at room temperature. Then the mixture was poured in water (30 mL), extracted with CH_2Cl_2 (2×20 mL), washed with water (2×20 mL) and dried over Na_2SO_4. Then the solvent was evaporated and the residue was purified by column chromatography on silica gel, eluting with CH_2Cl_2/petroleum ether (3:2). The yield of **15** was 8.6 mg (79%). ^{1}H NMR (600 MHz, $CDCl_3$, 303 K) δ ppm: -2.65 (s, 2H, NH), 7.83 (6H, m, Ph in Porphyrin), 8.00 (1H, t, *J* = 7.54 Hz, Pyrenyl), 8.0 (4H, m, C^{2}H Ethenyl and H in Pyrenyl), 8.27 (1H, d, *J* = 7.54 Hz, Pyrenyl), 8.30 (4H, m, Ph in Porphyrin), 8.47 (2H, m, Pyrenyl), 8.63 (1H, d, *J* = 9.44 Hz, Pyrenyl), 8.98 (1H, d, *J* = 7.91 Hz, Pyrenyl), 9.0 (4H, m, β-H in Porphyrin), 9.32 (2H, d, *J* = 4.48 Hz, β-H in Porphyrin), 9.72 (2H, d, *J* = 4.67 Hz, β-H in Porphyrin), 10.9 (1H, d, *J* = 15.78 Hz, C^{1}H Ethenyl), 10.17 (1H, s, *meso*-H in Porphyrin). ^{13}C NMR (150 MHz, $CDCl_3$, 303 K) δ ppm: 104.88, 117.81, 119.99, 123.18, 123.84, 125.05, 125.27, 125.32, 125.43, 125.54, 126.15, 126.86, 127.58, 127.71, 127.78, 128.15, 129.01, 131.05, 131.49, 131.63, 132.48, 132.59, 134.68, 141.11, 141.88. UV-Vis (CH_2Cl_2) λ_{max} ($A_{rel.}$) nm: 242 (0.33), 275(0.196), 348 (0.227), 418 (1.00), 516 (0.078), 566 (0.091), 656 (0.035).

*Zn(II) 5-(2-(pyrene-1-yl)ethenyl)-10,20-diphenylporphyrin (**16**).* 5-(2-(Pyrene-1-yl)ethenyl)-10,20-diphenylporphyrin (**15**) (8.6 mg, 0.012 mmol) was dissolved in chloroform (3.5 mL). Then the solution of $Zn(OAc)_2{\cdot}2H_2O$ (24 mg, 0.11 ммоль) in methanol (1.5 mL) was added and the mixture was heated to reflux for an 1 h. Then the mixture was poured in water (10 mL), extracted with CH_2Cl_2 (15 mL), washed with water (10 mL) and dried over Na_2SO_4. Then the mixture was passed through a silica plug and the solvent was evaporated yielding 5.8 mg (62%) of **16**. ^{1}H NMR (600 MHz, $CDCl_3$, 303 K) δ ppm: 7.82 (6H, m, Ph in Porphyrin), 8.00 (1H, t, *J* = 7.67 Hz, Pyrenyl), 8.1 (2H, m, Pyrenyl), 8.16 (2H, m, Pyrenyl), 8.20 (1H, d, *J* = 7.75 Hz, Pyrenyl), 8.29 (4H, m, Ph in Porphyrin), 8.41 (2H, m, C^{2}H Ethenyl and H in Pyrenyl), 8.60 (1H, d, *J* = 9.37 Hz, Pyrenyl), 8.94 (1H, d, *J* = 7.85 Hz, Pyrenyl), 9.1 (4H, m, β-H in Porphyrin), 9.36 (2H, d, *J* = 4.41 Hz, β-H in Porphyrin), 9.79 (2H, d, *J* = 4.59 Hz, β-H in Porphyrin), 9.96 (1H, d, *J* = 15.60 Hz, C^{1}H Ethenyl), 10.18 (1H, s, *meso*-H in Porphyrin). UV-Vis (CH_2Cl_2) λ_{max} ($A_{rel.}$) nm: 243 (0.861), 275 (0.523), 422 (1.00), 552 (0.090), 600 (0.074). LDI *m/z*: found 751.193, calc. for $[M+H]^+$ $C_{50}H_{31}N_4Zn$: 751.184.

Quantum-chemical calculations

Quantum-chemical calculations of geometry and electronic structure were made with the software package Gaussian 09W[55] using density functional theory (DFT) method with the hybrid correlation-exchange functional B3LYP. A full-electron 6-31G(d,p) basis set was used for the geometry optimizations, electrons of nickel and palladium atoms were rendered by the basis set with an effective potential for internal electrons LaNL2DZ.

The molecules were calculated in the dichloromethane solution using the polarized continuum (PCM) model. TD-DFT calculation of the electronic transitions were performed using WB97XD functional with DGDZVP basis set using the ground state geometry, calculated with B3LYP/6-31G(d,p).

Results and Discussion

Synthesis

In order to create a dyad with potential conjugation between components, catalytic cross-coupling reactions are the method of choice, and among them the Suzuki reaction is one of the most efficient. The nucleopilic substrate of the coupling was 1-pyreneboronic acid. Electrophilic partner was halogenated porphyrin. Porphyrin component for preparation of dyads was chosen to be 5,15-diphenylporphyrin (**1**) due to its free meso positions available for attachment of another component. To directly attach pyrene to porphyrin, the latter was brominated at *meso*-position with NBS in $CHCl_3$/MeOH. However, it should be noted that the bromination proceeds with low selectivity and a mixture of 5-bromo-10,20-diphenylporphyrin (**2**) along with 5,15-dibromo-10,20-diphenylporphyrin (**3**) was obtained even when using an excess of porphyrin (Scheme 1). Column chromatography was used to separate the mixture, although the low solubility of these compounds, especially the dibromo compound, complicates the process. The resulting 5-bromo-10,20-diphenylporphyrin (**2**) was then metalated with zinc acetate to give Zn(II) 5-bromo-10,20-diphenylporphyrin (**4**). Zinc complex is better to use than free base porphyrin in metal-catalyzed reactions. This is because the metal-free porphyrin acts as a ligand that can coordinate with the catalytic metal, and thus remove it from its active state.

Alternatively, the components of the dyad were linked *via* an ethene bridge. In this case, the electrophilic substrate used for the formation of the dyad was 5-(2-iodoethenyl)-10,20-diphenylporphyrin. This compound was prepared from 5,15-diphenylporphyrin using the Vilsmeier-Haack formylation followed by the Takai reaction (Scheme 1). Formylation of porphyrins is typically carried out with Ni(II), Cu(II) or Pd(II) complexes, as these are known to be robust and stable, remaining intact under the acidic conditions in the reaction. Nickel complexes were chosen because they were found to be most efficient for the subsequent Takai reaction. Ni(II) 5,15-diphenylporphyrin (**5**) was prepared by refluxing 5,15-diphenylporphyrin (**1**) with nickel acetate in DMF. Formylation was performed using the Vilsmeier-reagent $POCl_3$/DMF in 1,2-dichloroethane at 50 °C. The resulting Ni(II) 5-formyl-10,20-diphenylporphyrin (**6**) was obtained in 86% yield, and transformed to the Ni(II) 5-(2-iodoethenyl)-10,20-diphenylporphyrin (**7**) during the Takai reaction with $CrCl_2/CHI_3$ in 64% yield. In order to obtain other metal complexes as well as free base dyad, the nickel complex of the porphyrin precursor **7** was demetalated with trifluoroacetic acid in sulfuric acid yielding free base 5-(2-iodoethenyl)-10,20-diphenylporphyrin (**8**) with 57% yield.

Having in hand all the precursors, the Suzuki coupling of the halogenated porphyrins with 1-pyreneboronic acid (**9**) was elaborated. The porphyrin substrates often yielded

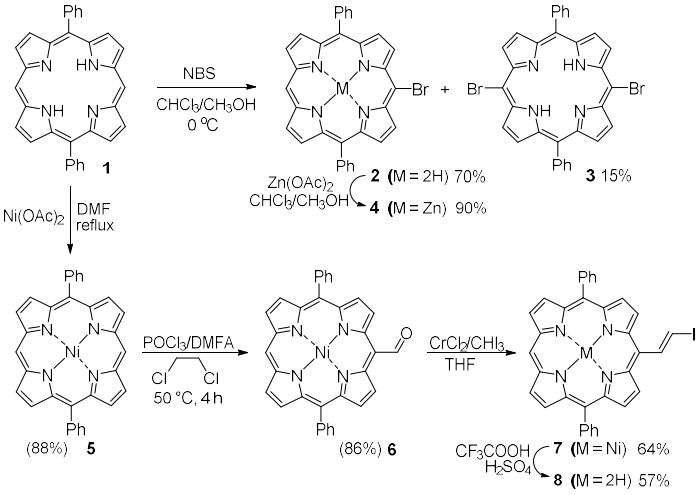

Scheme 1. Synthesis of the halogenated porphyrin substrates.

unsatisfactory results under standard cross-coupling conditions. This is due to the fact that porphyrins are unique substrates that require specialized synthetic techniques. Standard techniques have been developed for simple benzene substrates, but when applied to porphyrins, which differ significantly in their structure, they can lead to unsatisfactory results.[56] The specific conditions needed to be developed for each porphyrin substrate type. For the coupling or Zn(II) 5-bromo-10,20-diphenylporphyrin (**4**) with **9** various palladium catalysts ($Pd(PPh_3)_4$, $Pddba_2$/XPhos, $Pddba_2$/CyJohnPhos) were tested. The reaction conditions were optimized as follows: Cs_2CO_3 as a base in THF or 1,4-dioxane with addition of 4%vv H_2O at 60 °C for 24 h. The $Pd(PPh_3)_4$ led to extensive palladium black formation accompanied with side reaction of the hydrodebromination of the substrate **4** leading to the Zn(II) 5,15-diphenylporphyrin (**10**) as a major product. XPhos ligand performed far better than PPh_3, however, the conversion was low after 24 h, yielding 28% (by NMR) of the product **11**. CyJohnPhos was proved to be the most efficient, providing 71% isolated yield of the dyad **11** in these conditions (Scheme 2). Zinc can be easily removed from porphyrin, and the corresponding demetalation of the dyad was achieved in mild conditions with 0.4 %vv trifluoroacetic acid in chloroform solution for 10 min at 60 °C with 99% yield. The free base dyad **12** was then metalated with nickel acetate in refluxing DMF for 1 h to give the dyad **13** with 99% yield. Thus, three directly linked porphyrin – pyrene dyads **11**-**13** were obtained.

The Suzuki coupling of Ni(II) 5-(2-iodoethenyl)-10,20-diphenylporphyrin (**7**) with 1-pyreneboronic acid (**9**) was also optimized, as the iodo-ethenylporphyrin is a completely different electrophilic substrate with a higher activity towards oxidative addition to the palladium. A number of catalysts was tested, including those used in the synthesis of the directly linked dyad **11**. However, the results were not satisfactory. It was reported that $PdCl_2$dppf was successfully used in the Suzuki reaction of N-(2-iodoethenyl)benzamido derivatives in the synthesis of Alatamide.[57] We found that this catalyst was also efficient in coupling of the corresponding 2-iodoethenyl porphyrin substrate **7**. Coupling of **7** with **9** proceeded with K_3PO_4 as a base in dioxane/H_2O 5:1 at 40 °C for an hour, yielding

68% of the nickel dyad **14**. The dyad linked by ethene bridge is not so robust due to the presence of relatively reactive ethene double bond. An attempt to remove the nickel from the dyad under harsh conditions with sulfuric acid resulted in its destruction. Therefore, the demetalation was performed on the precursor **7**, and the free base dyad **15** was obtained using the Suzuki reaction from the corresponding free base iodo-ethenylporphyrin **8**. The Suzuki coupling of **8** with **9** was carried out at room temperature, and it took 8 hours to complete the reaction giving the corresponding dyad **15** with 79% yield. Then zinc complex of the dyad **16** was obtained by reaction of **15** with zinc acetate yielding the dyad **16** in 62% yield. Thus, three ethene linked porphyrin – pyrene dyads **14**-**16** were obtained.

NMR spectra

In the NMR spectra of the dyads characteristic signals of 5,15-diphenylporphyrin and pyrene units were clearly observed, but the resonances of protons are shifted compared to that of the precursors. All protons of pyrene are nonequivalent and appear as separate multiplets in the ^{1}H NMR spectra. In the spectra of ethene-bridged dyads there are two doublets of protons of the double bond of the bridge at 8.4 and 10 ppm. Resonances of both protons are significantly shifted downfield due to the influence of both neighboring aromatic fragments. The CH=CH bridge protons have a large J^3 coupling constant of *ca*. 16 Hz, characteristic of *trans*-ethene protons. Therefore, the *E*-configuration of the double bond was determined in the ethene-bridged dyads.

Properties of electronic absorption and luminescence spectra

UV-Vis absorption spectra of the dyads **11**-**16** contain absorption bands originated from both pyrene and porphyrin components (Figure 1). The shape and position of the pyrene bands in some dyads have changed significantly. The maxima of the porphyrin bands are bathochromically shifted relatively to that in the precursor porphyrins (Table 1). It can be clearly seen in detail on the overlay of the spectra of nickel complexes and their precursors (Figure 2a). Additionally, all bands are broader, and bands in the ethene bridged dyads **14**-**16** are shifted and broaden to a greater extent than those in the directly linked components **11**-**13**. The large spectral change can be clearly seen at the overlay of the spectra of ethene bridged dyads **15**, **16** and its porphyrin components: *meso*-vinyl-diphenyl porphyrin DPPCHCH$_2$ and its zinc complex ZnDPPCHCH$_2$ (Figure 2b). The reason for the bathochromic shift in the absorption bands of porphyrins is the influence of the pyrene chromophore. This influence is weaker in directly bridged dyads and stronger in ethene-bridged dyads. Comparing the spectra of these dyads with those of *meso*-vinyl porphyrins, we can conclude that the influence of the pyrene unit is significantly stronger than that of the ethene bridge. This points out on considerable interactions of components in the ethene bridged dyads.

All the dyads exhibited luminescence when irradiated at wavelengths corresponding to the absorption of both the pyrene and porphyrin components. The type of the luminescence, observed in solution at room temperature is fluorescence, as determined by the fast decay rate. The luminescence of the nickel dyads **13** and **14** is very weak in intensity, however, the dyad **14** exhibited relatively strong blue emission from the pyrene unit.

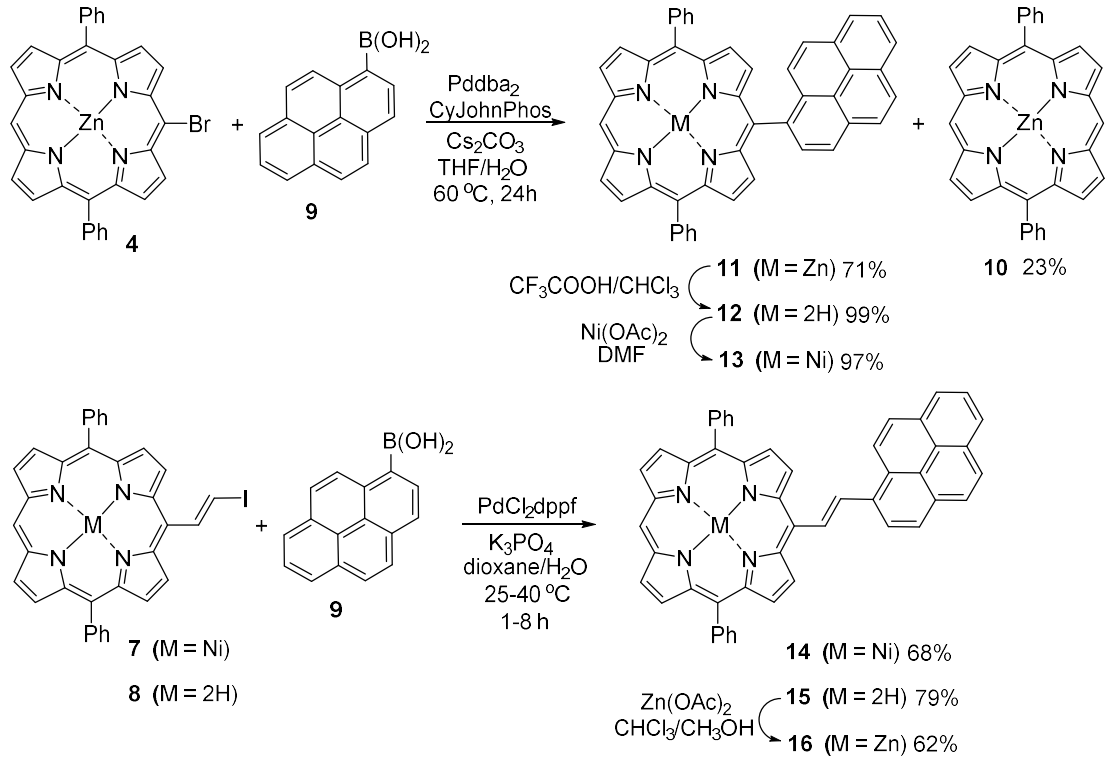

Scheme 2. Synthesis of the dyads of 5,15-diphenylporphyrin with pyrene.

Table 1. UV-Vis absorption spectra data.

Compound	Absorption bands, λ_{max}, nm [a]	
	Soret band	Q-bands
DPP (**1**)	412	508, 543, 580, 636
NiDPP (**5**)	403	519, 551
ZnDPP (**10**)	414	548, 591
NiDPPCHCHI (**7**)	419	533
$DPPCHCH_2$	413	511, 547, 588, 644
$ZnDPPCHCH_2$	414	545, 583
11	420	551, 590
12	413	541
13	409	521, 550
14	427	535, 583
15	418	516, 566, 656
16	422	552, 600

[a] recorded in CH_2Cl_2 at concentration 10^{-5} M;

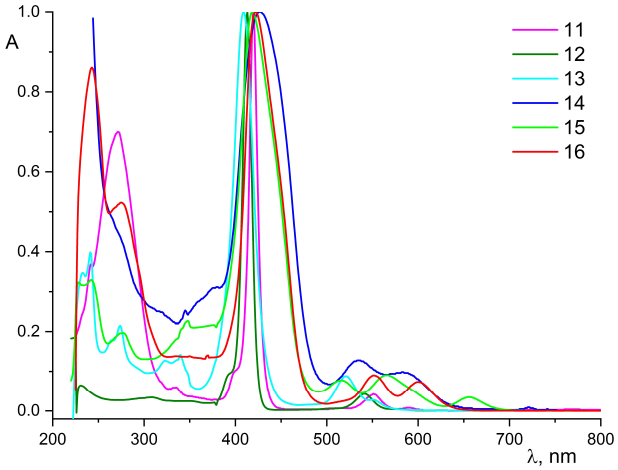

Figure 1. Normalized UV-Vis spectra of the dyads in CH_2Cl_2 at concentration of 10^{-5} M.

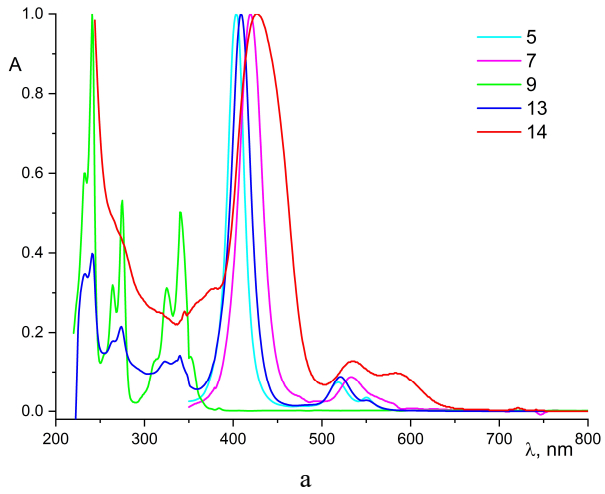

a

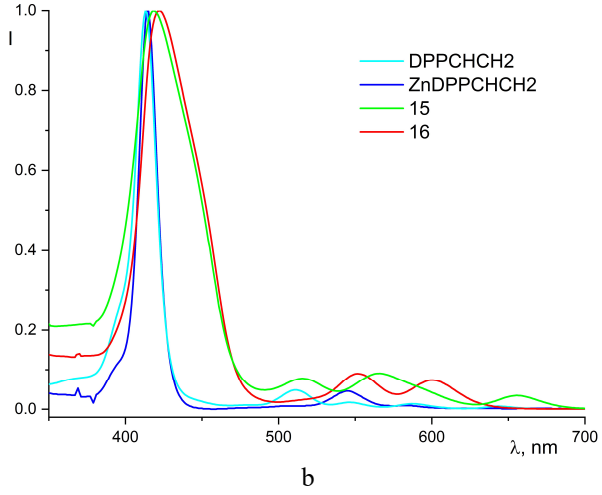

b

Figure 2. a) Normalized UV-Vis spectra of the nickel dyads **13, 14** and their starting components **5**, **7**, **9**; b) Normalized UV-Vis spectra of the ethene linked dyads **15, 16** and their *meso*-vinyl porphyrin components $DPPCHCH_2$, $ZnDPPCHCH_2$.

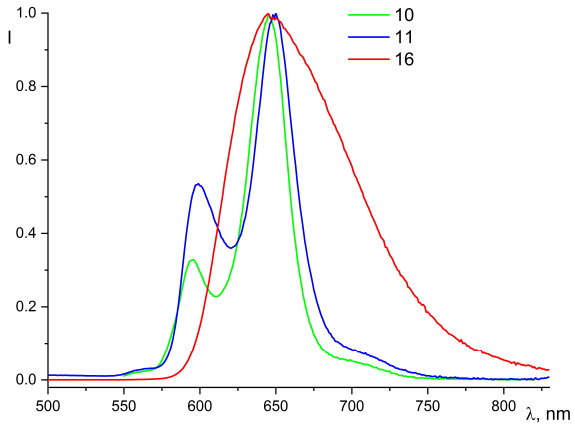

a

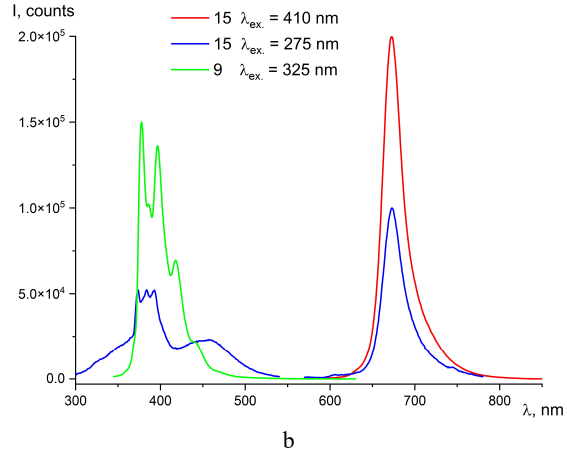

b

Figure 3. a) Normalized fluorescence spectra of zinc dyads **11**, **16** and its precursor **10**, excitation at 420 nm (**10**), 425 nm (**11**), 405 nm (**16**); b) Fluorescence spectra of the dyad **15** at two different excitation wavelengths and its precursor pyrene-boronic acid (**9**).

Table 2. Luminescence parameters of dyads **11-16**.

Compound	λ_{ex}[a], nm	λ_{em}[b], nm
10	420	595, 646
11	425	599, 649
13	410	667, 687
14	418	650, 713
15	410	673
16	405	648

[a]excitation wavelength; [b]maximum of emission wavelength

The fluorescent spectra of the directly linked zinc dyad **11** almost repeats that of the zinc porphyrin **10** with slightly bathochromically shifted maximum, while the band of the ethene linked zinc dyad **16** is considerably broaden (Figure 3a) in parallel to the corresponding broadening of the absorption bands. The fluorescence bands fairly correspond to the long wavelength absorption bands with the Stokes shift (Table 2). Excitation of both the zinc dyads **11** and **16** at the pyrene absorption wavelengths of 315-320 nm led to the major blue pyrene emission and minor red porphyrin emission. Excitation of the free base dyad **15** at the pyrene absorption band at 275 nm led to the dual blue pyrene and red porphyrin emission of almost equal intensity (Figure 3b). The porphyrin emission emerged probably due to the partial energy transfer, with a low degree of transfer in zinc dyads and a higher degree of transfer in free base and nickel dyads.

Thus, the porphyrin-pyrene dyads can produce emission from both chromophores. When the dyad is irradiated with UV light, blue light is emitted from the pyrene unit and red light from the porphyrin unit, which is due to the partial energy transfer from the excited pyrene to the porphyrin fragment in the dyad. An efficiency of the transfer is lower in the metal complexes in general, but the nickel dyad **13** represents exclusion. The presence of emission from both chromophores, as well as the ability to excite different fragments selectively, opens up possibilities for using these molecules in ratiometric sensors.

DFT studies of the dyads

Optimization of the geometry of the molecules **11-16** was performed by the B3LYP functional and 6-31G(d,p) basis set for light atoms and LanL2DZ for Ni, Zn. The structural characteristics of the dyads are similar for metal complexes and free bases. All direct dyads **11-13** feature almost orthogonally oriented porphyrin and pyrene fragments with no π-conjugation with each other (Figure 4). The dihedral angle between the C-C bond linking two fragments in **13** is about 85°. This leads to the lack of π-conjugation between the two parts of the molecule, and consequently, to their low level of interaction in the ground state. Contrary to the direct dyads, all the ethene-bridges dyads **14-16** feature a tendency towards a more coplanar arrangement of the fragments. The dihedral angle between the porphyrin and ethene bridge in **14** is 39°, which allows appreciable π-orbitals overlap between porphyrin and bridge leading to their π-electron conjugation. Such a conjugation leads to the interaction of the chromophores in the ground state, which can be responsible for the appreciable change in their optical spectral properties. TD-DFT calculations of the electronic transitions using the WB97XD functional and the DGDZVP basis set have revealed that the ethene bridged dyad **14** contains a second Soret band component that is bathochromically shifted by 25 nm (Figure 5). Both components overlap and form a broad intense absorption band with a half width of 50 nm in the blue range of the visible spectrum. The Q-band has been significantly broadened and has gained much higher intensity in the green-orange range, compared to that of the precursor **5**. The oscillator strength (f) of the Q-band at 533 nm was 0.005 in the spectrum of **5**, but it has 80-fold increased to 0.16 in the spectrum of **14**. In addition, a new band at 354 nm has emerged, corresponding to transitions between molecular orbitals spanning all units: pyrene, porphyrin, and ethene bridge. Therefore, TD-DFT calculations confirm that the intense and broad absorption spectrum of the ethene-bridged dyad results from strong intrechromophore interactions. The difference in the interaction between the components of the two types of dyads can be clearly seen in the plot of the frontier molecular orbitals (FMOs) (Figure 6). In dyad **13**, four Gouterman FMOs are retained, and two pyrene FMOs lie below and above. In dyad **14**, the HOMO and LUMO are centered on both chromophores and the ethene bridge. The original pyrene FMOs also contain some porphyrin-centered components.

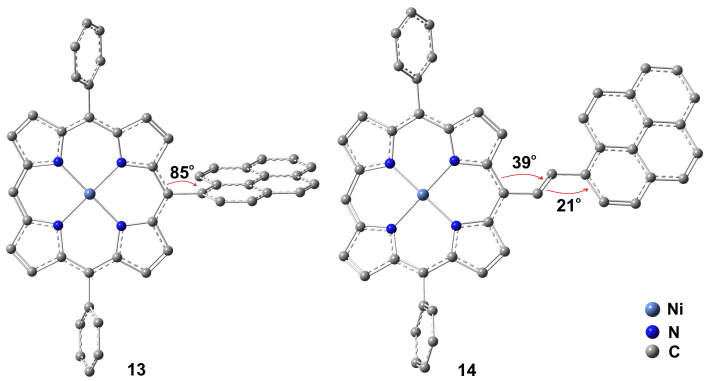

Figure 4. Geometry of the dyad **13** and **14** optimized by the DFT (B3LYP/6-31G(d,p)). Hydrogen atoms are omitted for clarity.

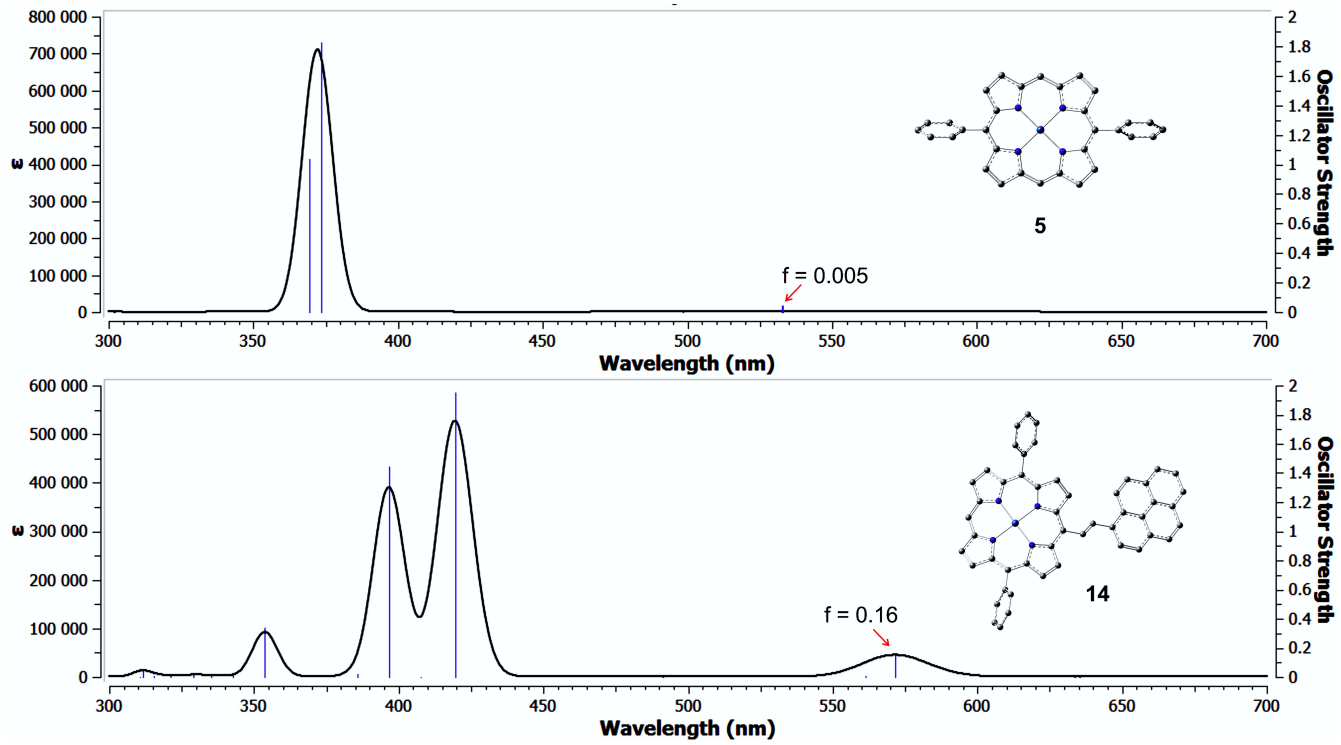

Figure 5. Absorption spectra of the dyad **14** and its precursor **5** calculated with TD-DFT (WB97XD/DGDZVP). Vertical blue lines correspond to the energy of transitions and their oscillator strength (f).

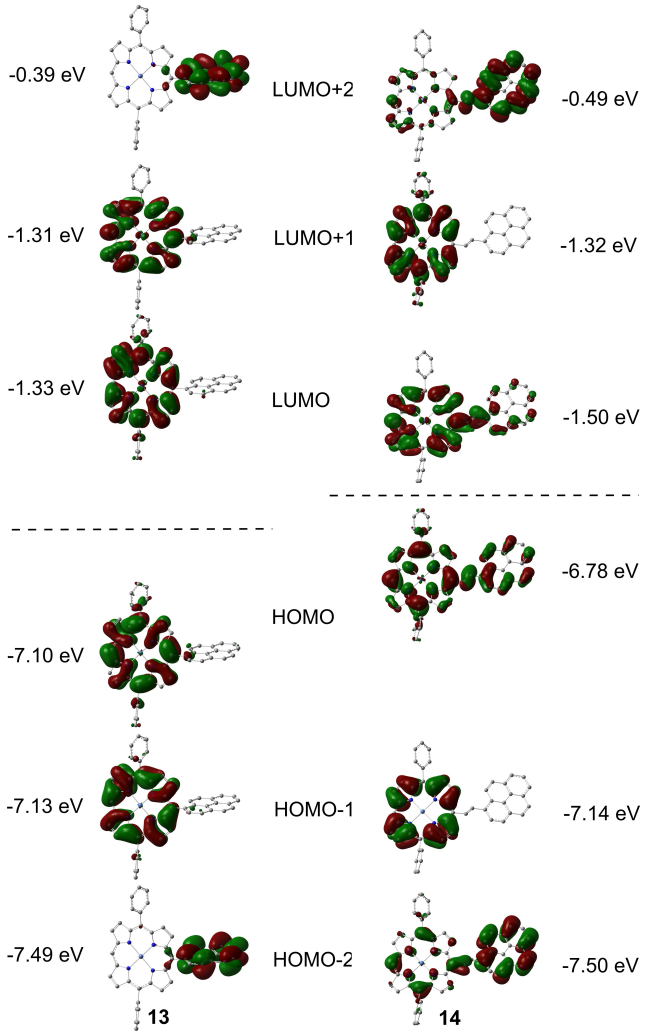

Figure 6. Plot of the frontier molecular orbitals of the dyad **13** and **14** and their energies calculated with the DFT (WB97XD/DGDZVP).

In conclusion, new 5,15-diphenylporphyrin-pyrene dyads were obtained. The dyads differ in the way of linking components: directly bonded and ethene bridged. The dyads were obtained in the form of free bases as well as nickel and zinc complexes. The absorption and fluorescence spectra as well as DFT calculations showed a lack of conjugation between the chromophores in the directly attached dyads due to the mutual almost orthogonal orientation of the porphyrin ring and the pyrene fragment. However, efficient interchromophore communication was observed in the ethene linked dyads, as was deducted from their optical spectral properties and confirmed by the DFT calculations. The irradiation of free base and zinc dyads resulted in strong fluorescence. The dyads feature red and blue emission regions which ratio depends on their structure and irradiation wavelength. The free base porphyrin-pyrene dyad features efficient excited energy transfer from the pyrene to the porphyrin unit, resulted in strong red porphyrin emission, while the zinc complexes possess strong green pyrene emission. Nickel complexes showed a very weak red luminescence and a strong blue luminescence from the pyrene chromophore in the ethene-bridged dyad, but weak blue emission in the direct dyad. Therefore, the excited pyrene chromophore was not completely quenched by the nickel porphyrinate component The obtained dyads could be of interest as potential photosensitizers and ratiometric luminescent sensors based on their tunable dual blue and red luminescence.

Acknowledgements. The reported study was funded by the Russian Science Foundation, grant 23-23-00561.

Author Contribution. Uliana Gerasimova: Investigation. Artemiy Ershov: Investigation. Alexander Kuvakin: Investigation. Andrey Chernyadiev: Investigation. Dmitriy Kuznetsov: Resources. Sergey Ryagin: Formal analysis; Validation. Ilya Zamilatskov: Visualization; Methodology; Investigation. Vladimir Tyurin: Conceptualization; Writing - Original Draft; Writing - Review & Editing; Supervision; Funding acquisition.

References

1. Ohira S., Bredas J.-L. *J. Mater. Chem.* **2009**, *19*, 7545–7550. DOI: 10.1039/b906337d.
2. Ryan A., Gehrold A., Perusitti R., Pintea M., Fazekas M., Locos O.B., Blaikie F., Senge M.O. *Eur. J. Org. Chem.* **2011**, *2011*, 5817–5844. DOI: 10.1002/ejoc.201100642.
3. Glowacka-Sobotta A., Wrotynski M., Kryjewski M., Sobotta L., Mielcarek J. *J. Porphyrins Phthalocyanines* **2019**, *23*, 1–10. DOI: 10.1142/s108842461850116x.
4. Dahlstedt E., Collins H.A., Balaz M., Kuimova M.K., Khurana M., Wilson B.C., Phillips D., Anderson H.L. *Org. Biomol. Chem.* **2009**, *7*, 897–904. DOI: 10.1039/b814792b.
5. Balaz M., Collins H.A., Dahlstedt E., Anderson H.L. *Org. Biomol. Chem.* **2009**, *7*, 874–888. DOI: 10.1039/b814789b.
6. Cho H.S., Jeong D.H., Yoon M.-C., Kim Y.H., Kim Y.R., Kim D., Jeoung S.C., Kim S.K., Aratani N., Shinmori H., Osuka A. *J. Phys. Chem. A* **2001**, *105*, 4200–4210. DOI: 10.1021/jp010385n.
7. Zaragoza-Galán G., Fowler M., Rein R., Solladié N., Duhamel J., Rivera E. *J. Phys. Chem. C* **2014**, *118*, 8280–8294. DOI: 10.1021/jp501445n.
8. Qi Q., Li R., Luo J., Zheng B., Huang K.-W., Wang P., Wu J. *Dyes Pigm.* **2015**, *122*, 199–205. DOI: 10.1016/j.dyepig.2015.06.019.
9. Fan Y., Huang Y., Jiang Y., Ning X., Wang X., Shan D., Lu X. *J. Colloid Interface Sci.* **2016**, *462*, 100–109. DOI: 10.1016/j.jcis.2015.09.063.
10. Lee H.S., Han J.H., Park J.H., Heo M.E., Hirakawa K., Kim S.K., Cho D.W. *Phys. Chem. Chem. Phys.* **2017**, *19*, 27123–27131. DOI: 10.1039/C7CP05211A.
11. Heo M.E., Lee Y.-A., Hirakawa K., Okazaki S., Kim S.K., Cho D.W. *Phys. Chem. Chem. Phys.* **2018**, *20*, 16386–16392. DOI: 10.1039/C8CP01870G.
12. Rojas-Montoya S.M., Vonlanthen M., Porcu P., Flores-Rojas G., Ruiu A., Morales-Morales D., Rivera E. *Dalton Trans.* **2019**, *48*, 10435–10447. DOI: 10.1039/C9DT00855A.
13. Sheng N., Zhu P.-H., Ma C.-Q., Jiang J.-Z. *Dyes Pigm.* **2009**, *81*, 91–96. DOI: 10.1016/j.dyepig.2008.09.009.
14. Li X., Lovell J.F., Yoon J., Chen X. *Nat. Rev. Clin. Oncol.* **2020**, *17*, 657–674. DOI: 10.1038/s41571-020-0410-2.
15. Zhang J., Yang C., Zhang R., Chen R., Zhang Z., Zhang W., Peng S.-H., Chen X., Liu G., Hsu C.-S., Lee, C.-S. *Adv. Funct. Mater.* **2017**, *27*, 1605094. DOI: 10.1002/adfm.201605094.
16. Yu Z.-H., Li X., Xu F., Hu X.-L., Yan J., Kwon N., Chen G.-R., Tang T., Dong X., Mai Y., Chen D., Yoon J., He X.-P., Tian H. *Angew. Chem. Int. Ed.* **2020**, *59*, 3658–3664. DOI: 10.1002/anie.201913506.
17. Li X., Lee S., Yoon J. *Chem. Soc. Rev.* **2018**, *47*, 1174–1188. DOI: 10.1039/C7CS00594F.
18. Park K.C., Cho J., Lee C.Y. *RSC Advances* **2016**, *6*, 75478–75481. DOI: 10.1039/C6RA17664J.
19. Zoltan T., Vargas F., Rivas C., Lopez V., Perez J., Biasutto A. *Scientia Pharmaceutica* **2010**, *78*, 767–790. DOI: 10.3797/scipharm.1003-13.
20. Hirakawa K., Harada M., Okazaki S., Nosaka Y. *Chem. Commun.* **2012**, *48*, 4770–4772. DOI: 10.1039/C2CC30880K.
21. Zhang Y., Yang, Liu F., Li K.A. *Analyt. Chem.* **2004**, *76*, 7336–7345. DOI: 10.1021/ac049477+.
22. Wu W., Wu W., Ji S., Guo H., Wang X., Zhao J. *Dyes Pigm.* **2011**, *89*, 199–211. DOI: 10.1016/j.dyepig.2010.01.020.
23. Sheng N., Liu D., Wu J., Gu B., Wang Z., Cui Y. *Dyes Pigm.* **2015**, *119*, 116–121. DOI: 10.1016/j.dyepig.2015.03.033.
24. Sheng N., Gu B., Ren B., Zhang J., Wang Y., Wang J., Sha J. *Dyes Pigm.* **2017**, *142*, 116–120. DOI: 10.1016/j.dyepig.2017.03.018.
25. Economopoulos S.P., Skondra A., Ladomenou K., Karousis N., Charalambidis G., Coutsolelos A.G., Tagmatarchis N. *RSC Adv.* **2013**, *3*, 5539–5546. DOI: 10.1039/C3RA40310F.
26. Wang C.-L., Chang Y.-C., Lan C.-M., Lo C.-F., Wei-Guang Diau E., Lin C.-Y. *Energy Environ. Sci.* **2011**, *4*, 1788–1795. DOI: 10.1039/C0EE00767F.
27. Lu J., Liu S., Li H., Shen Y., Xu J., Cheng Y., Wang M. *J. Mater. Chem. A* **2014**, *2*, 17495–17501. DOI: 10.1039/C4TA03435J.
28. Chao Y.-H., Jheng J.-F., Wu J.-S., Wu K.-Y., Peng H.-H., Tsai M.-C., Wang C.-L., Hsiao Y.-N., Wang C.-L., Lin C.-Y., Hsu C.-S. *Adv. Mater.* **2014**, *26*, 5205–5210. DOI: 10.1002/adma.201401345.
29. Wu C.-H., Chen M.-C., Su P.-C., Kuo H.-H., Wang C.-L., Lu C.-Y., Tsai C.-H., Wu C.-C., Lin C.-Y. *J. Mater. Chem. A* **2014**, *2*, 991–999. DOI: 10.1039/C3TA14208F.
30. Prakash K., Sudhakar V., Sankar M., Krishnamoorthy K. *Dyes Pigm.* **2019**, *160*, 386–394. DOI: 10.1016/j.dyepig.2018.08.029.
31. Li C.-H., Chang C.-C., Hsiao Y.-H., Peng S.-H., Su Y.-J., Heo S.-W., Tajima K., Tsai M.-C., Lin C.-Y., Hsu C.-S. *ACS Appl. Mater. Interfaces* **2019**, *11*, 1156–1162. DOI: 10.1021/acsami.8b19060.

32. Sheng N., Yuan Z., Wang J., Chen W., Sun J., Bian Y. *Dyes Pigm.* **2012**, *95*, 627–631. DOI: 10.1016/j.dyepig.2012.06.003.
33. Tanaka K., Ohashi W., Inafuku K., Shiotsu S., Chujo Y. *Dyes Pigm.* **2020**, *172*, 107821. DOI: 10.1016/j.dyepig.2019.107821.
34. Gray V., Börjesson K., Dzebo D., Abrahamsson M., Albinsson B., Moth-Poulsen K. *J. Phys. Chem. C* **2016**, *120*, 19018–19026. DOI: 10.1021/acs.jpcc.6b06298.
35. Managa M., Achadu O.J., Nyokong T. *Dyes Pigm.* **2018**, *148*, 405–416. DOI: 10.1016/j.dyepig.2017.09.031.
36. D'Souza F., Maligaspe E., Sandanayaka A.S.D., Subbaiyan N.K., Karr P.A., Hasobe T., Ito O. *J. Phys. Chem. A* **2010**, *114*, 10951–10959. DOI: 10.1021/jp1028195.
37. K. C. C. B., Das S.K., Ohkubo K., Fukuzumi S., D'Souza F. *Chem. Commun.* **2012**, *48*, 11859–11861. DOI: 10.1039/C2CC36262G.
38. Zhong Q., Diev V.V., Roberts S.T., Antunez P.D., Brutchey R.L., Bradforth S.E., Thompson M.E. *ACS Nano* **2013**, *7*(4), 3466–3475. DOI: 10.1021/nn400362e.
39. Elouarzaki K., Fisher A.C., Lee J.-M. *J. Mater. Chem. A* **2017**, *5*, 8927–8932. DOI: 10.1039/C7TA01525A.
40. Garrido M., Volland M.K., Münich P.W., Rodríguez-Pérez L., Calbo J., Ortí E., Herranz M.Á., Martín N., Guldi D.M. *J. Am. Chem. Soc.* **2020**, *142*, 1895–1903. DOI: 10.1021/jacs.9b10772.
41. Ayyavoo K., Velusamy P. *New J. Chem.* **2021**, *45*, 10997–11017. DOI: 10.1039/D1NJ00158B.
42. Birin K.P., Abdulaeva I.A., Polivanovskaia D.A., Martynov A.G., Shokurov A.V., Gorbunova Y.G., Tsivadze A.Y. *Dyes Pigm.* **2021**, *186*, 109042. DOI: 10.1016/j.dyepig.2020.109042.
43. Shepeleva I.I., Birin K.P., Polivanovskaia D.A., Martynov A.G., Shokurov A.V., Tsivadze A.Y., Selektor S.L., Gorbunova Y.G. *Chemosensors* **2023**, *11*, 43. DOI: 10.3390/chemosensors 11010043.
44. Kilså K., Kajanus J., Macpherson A.N., Mårtensson J., Albinsson B. *J. Am. Chem. Soc.* **2001**, *123*, 3069–3080. DOI: 10.1021/ja003820k.
45. Diev V.V., Schlenker C.W., Hanson K., Zhong Q., Zimmerman J.D., Forrest S.R., Thompson M.E. *J. Org. Chem.* **2012**, *77*, 143–159. DOI: 10.1021/jo201490y.
46. Orlova E.A., Romanenko Y.I., Tyurin V.S., Shkirdova A.O., Belyaev E.S., Grigoriev M.S., Koifman O.I., Zamilatskov I.A. *Macroheterocycles* **2022**, *15*, 139–146. DOI: 10.6060/mhc224638z.
47. Shkirdova A.O., Tyurin V.S., Chernyadyev A.Y., Zamilatskov I.A. *New J. Chem.* **2024**, *48*, 16481–16490. DOI: 10.1039/D4NJ02811B.
48. Belyaev E.S., Shkirdova A.O., Kozhemyakin G.L., Tyurin V.S., Emets V.V., Grinberg V.A., Cheshkov D.A., Ponomarev G.V., Tafeenko V.A., Radchenko A.S., Kostyukov A.A., Egorov A.E., Kuzmin V.A., Zamilatskov I.A. *Dyes Pigm.* **2021**, *191*, 109354. DOI: 10.1016/j.dyepig.2021.109354.
49. Andreeva V.D., Ponomarev G.V., Shkirdova A.O., Tyurin V.S., Zamilatskov I.A. *Macroheterocycles* **2021**, *14*, 201–207. DOI: 10.6060/mhc213990z.
50. Littler B.J., Miller M.A., Hung C.-H., Wagner R.W., O'Shea D.F., Boyle P.D., Lindsey J.S. *J. Org. Chem.* **1999**, *64*, 1391–1396. DOI: 10.1021/jo982015+.
51. DiMagno S.G., Lin V.S.Y., Therien M.J. *J. Org. Chem.* **1993**, *58*, 5983–5993. DOI: 10.1021/jo00074a027.
52. Shi X., Amin S.R., Liebeskind L.S. *J. Org. Chem.* **2000**, *65*, 1650–1664. DOI: 10.1021/jo9912799.
53. Dahms K., Senge M.O., Bakri Bakar M. *Eur. J. Org. Chem.* **2007**, *2007*, 3833–3848. DOI: 10.1002/ejoc.200700380.
54. Arnold D.P., Hartnell R.D. *Tetrahedron* **2001**, *57*, 1335–1345. DOI: 10.1016/S0040-4020(00)01102-9.
55. Frisch M.J., Trucks G.W., Schlegel H.B., Scuseria G.E., Robb M.A., Cheeseman J.R., Scalmani G., Barone V., Mennucci B., Petersson G.A., Nakatsuji H., Caricato M., Li X., Hratchian H.P., Izmaylov A.F., Bloino J., Zheng G., Sonnenberg J.L., Hada M., Ehara M., Toyota K., Fukuda R., Hasegawa J., Ishida M., Nakajima T., Honda Y., Kitao O., Nakai H., Vreven T., Montgomery J.A.J., Peralta J.E., Ogliaro F., Bearpark M., Heyd J.J., Brothers E., Kudin K.N., Staroverov V.N., Keith T., Kobayashi R., Normand J., Raghavachari K., Rendell A., Burant J.C., Iyengar S.S., Tomasi J., Cossi M., Rega N., Millam J.M., Klene M., Knox J.E., Cross J.B., Bakken V., Adamo C., Jaramillo J., Gomperts R., Stratmann R.E., Yazyev O., Austin A.J., Cammi R., Pomelli C., Ochterski J.W., Martin R.L., Morokuma K., Zakrzewski V.G., Voth G.A., Salvador P., Dannenberg J.J., Dapprich S., Daniels A.D., Farkas O., Foresman J.B., Ortiz J.V., Cioslowski J., Fox D.J. *Gaussian 09, Revision D.01*, Gaussian, Inc., Wallingford CT, **2013**.
56. Hiroto S., Miyake Y., Shinokubo H. *Chem. Rev.* **2017**, *117*, 2910–3043. DOI: 10.1021/acs.chemrev.6b00427.
57. Sambaiah M., Thota P., Kottawar S.S., Yennam S., Shiva Kumar K., Behera M. *ChemistrySelect* **2021**, *6*, 5406–5410. DOI: 10.1002/slct.202101093.

Received 27.10.2024
Accepted 22.11.2024